



Cite this: *Med. Chem. Commun.*,
2019, 10, 2161

Dual-target inhibitors of mycobacterial aminoacyl-tRNA synthetases among *N*-benzylidene-*N'*-thiazol-2-yl-hydrazines†

Oksana P. Kovalenko,^a Galyna P. Volynets,^b Mariia Yu. Rybak,^a Sergiy A. Starosyla,^b Olga I. Gudzera,^a Sergiy S. Lukashov,^b Volodymyr G. Bdzholo,^b Sergiy M. Yarmoluk,^b Helena I. Boshoff^c and Michael A. Tkalo^a

Effective treatment of tuberculosis is challenged by the rapid development of *Mycobacterium tuberculosis* (*Mtb*) multidrug resistance that presumably could be overcome with novel multi-target drugs. Aminoacyl-tRNA synthetases (AARSs) are an essential part of protein biosynthesis machinery and attractive targets for drug discovery. Here, we experimentally verify a hypothesis of simultaneous targeting of structurally related AARSs by a single inhibitor. We previously identified a new class of mycobacterial leucyl-tRNA synthetase inhibitors, *N*-benzylidene-*N'*-thiazol-2-yl-hydrazines. Molecular docking of a library of novel *N*-benzylidene-*N'*-thiazol-2-yl-hydrazine derivatives into active sites of *M. tuberculosis* LeuRS (*Mtb*LeuRS) and MetRS (*Mtb*MetRS) resulted in a panel of the best ranking compounds, which were then evaluated for enzymatic potency. Screening data revealed 11 compounds active against *Mtb*LeuRS and 28 compounds active against *Mtb*MetRS. The hit compounds display dual inhibitory potency as demonstrated by IC_{50} values for both enzymes. Compound **3** is active against *Mtb* H37Rv cells in *in vitro* bioassays.

Received 4th July 2019,
Accepted 9th November 2019

DOI: 10.1039/c9md00347a

rsc.li/medchemcomm

Introduction

Tuberculosis is one of the deadliest human diseases and public problems throughout the world. The main problem of tuberculosis treatment is the rapid development of *Mycobacterium tuberculosis* (*Mtb*) multidrug resistance that stimulates the search for antibiotics with novel mechanisms of action as well as identification of novel targets for anti-tuberculosis treatment. The current outline of promising drugs and treatment opportunities has been recently reviewed.^{1–3} In the last decade, multi-target drugs have attracted much attention for the treatment of diseases associated with drug resistance.⁴ According to the strategy “one target–one drug”, which is the commonly favored approach in drug development, the application of highly

specific drugs diminishes the risk of side effects due to off-target effects. However, biological systems demonstrate resilience to single-point perturbations.⁵ Multi-target drugs are considered to reduce resistance emergence, a considerable challenge in drug discovery.

Aminoacyl-tRNA synthetases (AARSs) play a pivotal role in living cells and hence represent promising drug targets for antibiotic development.^{6–10} They catalyse the coupling of amino acids to their cognate tRNAs, providing aminoacyl-tRNA substrates for protein biosynthesis. The aminoacylation reaction starts with amino acid activation to generate an aminoacyl-adenylate intermediate (AA-AMP), followed by transfer of the amino acid moiety to the 3' end of its cognate tRNA, resulting in aminoacyl-tRNA formation. Most prokaryotic cells possess 20 different AARSs, one for each cognate amino acid–tRNA pair. All known AARSs are divided into two structural classes. Within each class, enzymes share a catalytic domain with a common fold that binds substrates for the aminoacylation reaction: amino acid, ATP and 3'-terminus of tRNA.¹¹ Simultaneous targeting of AARS enzymes by a cocktail of two AARS inhibitors reportedly overcame the considerable resistance liabilities of *Staphylococcus aureus* associated with inhibitors acting against a single AARS.¹² Multi-targeting of structurally related AARSs by a single inhibitor is assumed,^{6,10,12} but experimental data is missing.

Specificity of the AA-AMP formation in the first step consisting of the aminoacylation reaction strictly depends on

^a Department of Protein Synthesis Enzymology, Institute of Molecular Biology and Genetics, The NAS of Ukraine, 150 Zabolotnogo St, 03143 Kyiv, Ukraine.

E-mail: o.p.kovalenko@imbg.org.ua, o.p.kovalenko11@gmail.com;

Fax: +38 044 5260759; Tel: +38 044 5265589

^b Department of Medicinal Chemistry, Institute of Molecular Biology and Genetics, The NAS of Ukraine, 150 Zabolotnogo St, 03143 Kyiv, Ukraine

^c Tuberculosis Research Section, Laboratory of Clinical Immunology and Microbiology, National Institute of Allergy and Infectious Disease, National Institute of Health, 5601 Fishers Lane, MSC 9806, Bethesda, MD 20892-9806, Maryland, USA

† Electronic supplementary information (ESI) available. See DOI: 10.1039/c9md00347a

proper binding of the cognate amino acid within the active site of an AARS enzyme. Competitive inhibitors, mimicking the AA-AMP intermediate, usually display strong inhibitory potency against the target AARS [reviewed in ref. 10]. In

contrast, potential dual-target inhibitors would be compatible with the active sites of two AARSs. The binding affinity of such an inhibitor for a particular enzyme is expected to be compromised, compared to cognate aminoacyl-adenylate.

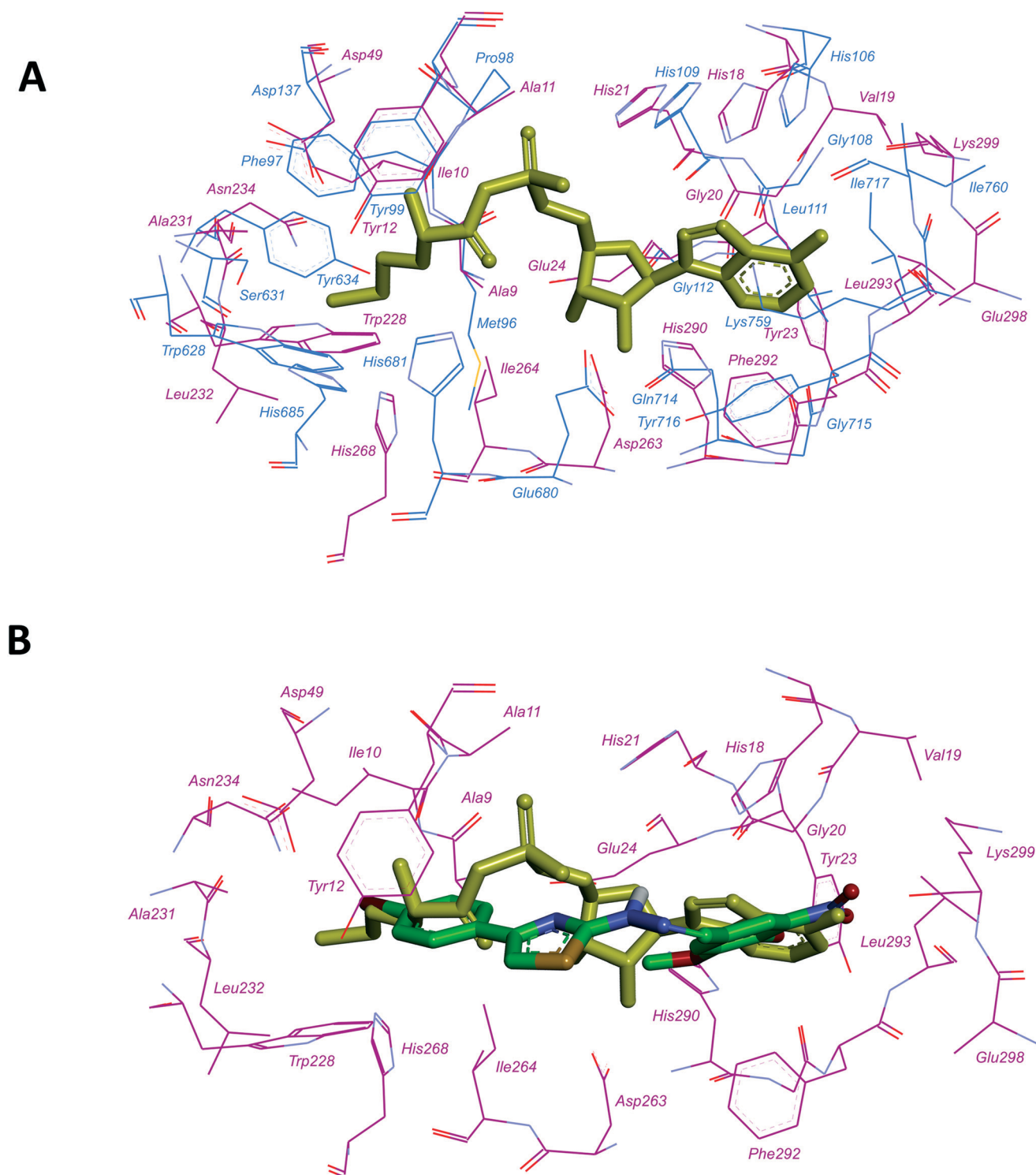


Fig. 1 Aminoacyl-adenylate binding pockets of *M. tuberculosis* LeuRS and MetRS. A. Superposition of the aminoacyl-adenylate binding pockets of *MtbLeuRS* (homology model)²⁰ and *MtbMetRS* (PDB: 6AX8). Carbon atoms of *MtbLeuRS* are coloured dark magenta, methionyl-adenylate is coloured yellow; B. docked pose of compound **1** in the active site of *MtbMetRS*. Colour scheme is the same as that in A. Carbon atoms of compound **1** are coloured green.

Nevertheless, we hypothesized that the exclusion of the amino acid-binding pocket from the design of a dual-target inhibitor would yield compounds exhibiting too broad specificity. Such inhibitors would likely target several ATP-binding proteins, not only aminoacyl-tRNA synthetases, which could result in unpredictable and significant off-target effects. For this reason, binding in the amino acid pocket of the active sites would enhance the on-target selectivity of a universal inhibitor.

Here, we report a strategy that yielded small molecular inhibitors capable of targeting two *M. tuberculosis* AARSs, leucyl-tRNA synthetase (*MtbLeuRS*) and methionyl-tRNA synthetase (*MtbMetRS*), simultaneously. Leucyl-, isoleucyl-, valyl-, and methionyl-tRNA synthetases share a well conserved overall structure and belong to the Ia subclass.¹³ They are known to effectively activate near-cognate proteinogenic and nonproteinogenic amino acids, demonstrating insufficient discrimination capability toward structurally related amino acids.^{14–18} Docking and molecular dynamics results displayed preferential binding of noncognate homocysteinyl-adenylate in similar positions in all four Ia subclass AARSs, suggesting marked structural resemblance between their active sites.¹⁹ Hence, this enzyme group is a promising potential target for the design of dual-target inhibitors.

Derivatives of *N*-benzylidene-*N'*-thiazol-2-yl-hydrazine have been previously identified as a chemical class of mycobacterial leucyl-tRNA synthetase (*MtbLeuRS*) inhibitors.²⁰ We conjectured that *M. tuberculosis* LeuRS inhibitors could potentially bind to and inhibit at least one of another Ia subclass AARS. In this respect, methionyl-tRNA synthetase (MetRS) is of particular interest because it catalyses not only the charging of elongator tRNA^{Met} but also of initiator tRNA^{FMet}. MetRS is a validated molecular target for drug design against protozoa, staphylococci, *Giardia intestinalis*, *Clostridium difficile*, and *Pseudomonas aeruginosa*.^{21–27} Recently, the crystal structure of the mycobacterial MetRS (*MtbMetRS*) has been reported making this enzyme of great interest in the structure-based design of antitubercular drugs.^{28,29}

Results and discussion

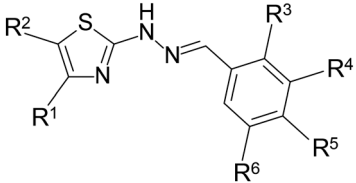
We compared the aminoacyl-adenylate binding pockets of *MtbMetRS* (PDB accession code: 6AX8) and *MtbLeuRS* (homology model, obtained by us earlier²⁰) and revealed their striking structural resemblance (Fig. 1A). Molecular docking calculations indicated similar binding modes of 4-[[4-(4-bromophenyl)-thiazol-2-yl]hydrazonomethyl]-2-methoxy-6-nitrophenol (compound 1)²⁰ to both active sites: 2-methoxy-6-nitrophenyl interacted with the adenine-binding region and the 4-substituted phenyl ring occupied the amino acid binding pocket (Fig. 1B and ESI† Fig. S1-1), suggesting that *MtbMetRS* could be a probable target for *N*-benzylidene-*N'*-thiazol-2-yl-hydrazine derivatives.

We performed molecular docking of a preselected library of *N*-benzylidene-*N'*-thiazol-2-yl-hydrazine derivatives (334

compounds) into the active sites of *MtbLeuRS* and *MtbMetRS* using the DOCK program as described previously.²⁰ According to the docking results (score values and bonding interactions) and visual analysis of the bound compounds (complementarity between ligand and receptor surfaces, the correctness of torsion angles, stacking interactions, etc.), a panel of the 35 best ranking novel compounds was evaluated for enzymatic potency against *MtbLeuRS* and *MtbMetRS*. Additionally, compounds 1 and 2, previously identified as the most potent inhibitors of *MtbLeuRS*, were subjected to evaluation of their dual-targeting capability.

MtbLeuRS (gene ID: 887040) and *MtbMetRS* (gene ID: 886050) were recombinantly expressed in *E. coli* cells and purified. The prepared enzymes were >90% pure as judged by SDS-PAGE followed by staining with Coomassie Brilliant Blue (shown in Fig. S3-1†). The *N*-benzylidene-*N'*-thiazol-2-yl-hydrazine derivatives were synthesized according to the general procedure previously reported by our group.²⁰ The representative structures of the compounds were confirmed with spectral data (¹H NMR and ¹³C NMR), and their purity was checked by chromatographic techniques (HPLC-MS). All selected compounds were dissolved in DMSO and screened for inhibitory activity against *MtbLeuRS* and *MtbMetRS* in aminoacylation assays (Table 1). The aminoacyl-tRNA synthetase activity was determined by monitoring the level of inorganic pyrophosphate released in the aminoacylation reaction. A coupled enzyme, inorganic pyrophosphatase, was present in the reaction mixture to convert the pyrophosphate molecule into two inorganic phosphate molecules. The phosphate concentration was measured using the BIOMOL® GREEN reagent (Enzo Life Sciences). Control incubations revealed that 10 compounds affected the steps downstream of the aminoacylation reaction mainly by attenuating the BIOMOL® GREEN signal (up to 35%) (ESI† Table S1). These compounds were eliminated from the investigation based on this assay interference. Nevertheless, all these compounds, except compound 8, demonstrated substantial inhibition of *MtbMetRS* (over 80%), and two of them, compounds 2 and 25, effectively inhibited the *MtbLeuRS* activity, suggesting that these compounds could be considered to show over 50% inhibition in screening assays. Excluding these compounds, there were nine potential inhibitors for *MtbLeuRS* and 18 for *MtbMetRS* with an inhibition cut-off taken as 50%. Taken together, screening data revealed 11 compounds active against *MtbLeuRS* and 28 compounds active against *MtbMetRS* (Fig. 2), suggesting that *MtbMetRS* is as relevant a target for *N*-benzylidene-*N'*-thiazol-2-yl-hydrazines as *MtbLeuRS*.

Analysis of the compounds' chemical structures indicated that the phenyl group was preferentially required as the R¹ substituent to improve efficiency against *MtbLeuRS*, whereas the methyl group as the R¹ substituent was also commonly found in compounds showing significant inhibition of *MtbMetRS* activity. Notably, all *MtbLeuRS* inhibitors are capable of reducing the *MtbMetRS* activity, demonstrating that they exhibit dual-targeted potency.

Table 1 *In vitro* structure–activity relationships of *N*-benzylidene-*N'*-thiazol-2-yl-hydrazines


Compound number	R ¹	R ²	R ³	R ⁴	R ⁵	R ⁶	Inhibition (%)	
							<i>MtbLeuRS</i>	<i>MtbMetRS</i>
1 ^a	C ₆ H ₄ -4-Br	H	H	NO ₂	OH	OCH ₃	113 ± 14 (5)	110 ± 6 (3)
2	C ₆ H ₄ -4-NO ₂	H	H	NO ₂	OH	OCH ₃	103 ± 9 (5)	94 ± 23 (4)
3	C ₆ H ₄ -4-F	H	H	Br	OCH ₃	H	109 ± 3 (2)	121 ± 8 (2)
4	C ₆ H ₃ -2,4-dCl	H	H	H	C(O)OH	H	101 ± 4 (2)	92 ± 4 (2)
5	C ₆ H ₄ -3-NO ₂	H	Br	H	H	H	80 ± 12 (2)	93 ± 10 (2)
6	C ₆ H ₄ -3-NO ₂	H	H	OC ₆ H ₅	H	H	11 ± 15 (2)	65 ± 15 (2)
7	C ₆ H ₄ -3-NO ₂	H	H	H	C ₂ H ₅	H	3 ± 23 (2)	27 ± 9 (2)
8 ^a	C ₆ H ₅	H	H	NO ₂	OH	H	53 ± 10 (2)	72 ± 16 (2)
9 ^a	C ₆ H ₅	CH ₃	H	OH	H	H	65 ± 18 (2)	112 ± 13 (2)
10 ^a	C ₆ H ₅	H	H	H	N(CH ₃)CH ₃	H	65 ± 18 (2)	122.7 ± 0.3 (2)
11	C ₆ H ₅	H	OH	H	H	H	7 ± 8 (2)	51 ± 4 (2)
12	3-Pyridyl	H	OCH ₃	H	H	OCH ₃	74 ± 4 (2)	115 ± 13 (2)
13	CH ₂ C(O)OC ₂ H ₅	H	H	H	C(O)OH	H	12 ± 4 (2)	22 ± 6 (2)
14	CH ₃	C(O)OC ₂ H ₅	CF ₃	H	H	H	34 ± 3 (2)	45 ± 4 (2)
15	CH ₃	C(O)OC ₂ H ₅	H	Br	OH	Br	55 ± 4 (2)	51 ± 17 (4)
16	CH ₃	C(O)OC ₂ H ₅	H	Br	OH	OCH ₃	54 ± 9 (2)	94 ± 5 (2)
17 ^a	CH ₃	C(O)OC ₂ H ₅	H	H	Br	H	39 ± 8 (2)	111 ± 6 (2)
18	CH ₃	C(O)OC ₂ H ₅	Br	H	H	H	67 ± 15 (2)	99 ± 13 (2)
19	CH ₃	C(O)OC ₂ H ₅	H	H	C(O)OH	H	-7 ± 11 (2)	6 ± 8 (2)
20	CH ₃	C(O)OC ₂ H ₅	H	OH	H	H	1 ± 2 (2)	71 ± 11 (2)
21	CH ₃	C(O)OC ₂ H ₅	H	H	H	H	19 ± 1 (2)	73 ± 13 (2)
22 ^a	CH ₃	C(O)OCH ₃	H	H	Br	H	46 ± 1 (2)	88 ± 18 (2)
23	CH ₃	C(O)OCH ₃	H	H	C(O)OH	H	12 ± 1 (2)	-11 ± 3 (2)
24	CH ₃	C(O)OCH ₃	H	H	NO ₂	H	88 ± 1 (2)	75 ± 12 (3)
25 ^a	CH ₃	C(O)CH ₃	H	OCH ₃	OCH ₂ C ₆ H ₄ -2-Cl	H	87 ± 21 (5)	113 ± 3 (2)
26	CH ₃	C(O)CH ₃	H	H	OC ₂ H ₅	H	20 ± 11 (2)	53 ± 0 (2)
27	CH ₃	CH ₃	H	H	OCH ₃	H	1 ± 10 (2)	1 ± 8 (2)
28	CH ₃	H	OCH ₃	OCH ₃	H	H	17 ± 8 (3)	25 ± 12 (2)
29	CH ₃	H	H	H	C(O)OH	H	-4 ± 17 (2)	-22 ± 2 (2)
30	CH ₃	H	H	H	NO ₂	H	20 ± 6 (2)	92 ± 3 (2)
31 ^a	H	H	H	OCH ₃	OC(O)C ₆ H ₃ -2,4-dCl	H	73 ± 16 (2)	142 ± 2 (2)
32 ^a	H	H	H	Br	OCH ₂ C ₆ H ₅	OCH ₃	55 ± 6 (2)	106 ± 1 (2)
33 ^a	H	H	H	OCH ₃	OCH ₂ C ₆ H ₄ -2-Cl	H	64 ± 1 (2)	102 ± 2 (2)
34	H	H	H	Br	OCH ₃	H	29 ± 11 (2)	90 ± 23 (4)
35	CH ₃	H	OH	H	H	Br	39 ± 3 (2)	113 ± 11 (2)
36	H	H	H	OCH ₃	OC ₆ H ₁₃	H	47 ± 6 (2)	62 ± 5 (2)
37	H	H	NO ₂	H	H	H	45 ± 35 (4)	51 ± 25 (4)

Compounds were tested at a concentration of 100 μM. The inhibition values are reported as mean ± standard deviation. The number of replicates is in parentheses. ^a Compounds that affected the steps downstream of the aminoacylation reaction in the assays (inorganic pyrophosphatase activity and/or development of BIOMOL® GREEN signal).

The compounds found to result in at least 80% inhibition of activity of both *MtbLeuRS* and *MtbMetRS* were further analysed to determine IC₅₀ values (Table 2). All compounds demonstrated no remarkable enzyme-dependent difference in inhibition activity, while they varied from one to another in potency by 2–5-fold. Compounds 2 and 5 inhibited both enzymes with IC₅₀ values below 10 μM. The potency of compound 3 was slightly lower (IC₅₀ values of 12.5 and 10.7 μM for *MtbLeuRS* and *MtbMetRS*, respectively). Compound 4 demonstrated markedly increased IC₅₀ values, suggesting the requirement of at least a single substitution at R³ or R⁴ with a bromine atom or

methoxy group for improved inhibitory activity against both enzymes.

To get some insight into the role of the phenyl ring as an R¹ substituent, we evaluated the inhibition potency of compounds 3a, 5a and 5b, which differ from the corresponding compounds 3 and 5 only in their R¹ substituent. According to the docking results, these compounds were ranked lower from the best ranking analogues. Substitution of the 4-fluoro-phenyl group (compound 3) with the methyl group (compound 3a) led to a severe decrease in the targeting capacity toward both AARs. Compound 29, which differs from compound 4 in terms of

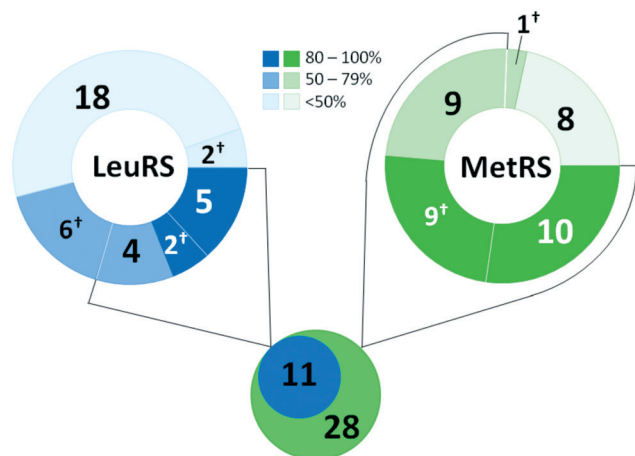


Fig. 2 Summary of screening. Ranges of inhibition of *M. tuberculosis* LeuRS and MetRS activity, the number of compounds within the scope and the total number of compounds with inhibition activity above 50% are shown. †The number of compounds affected the steps downstream of the aminoacylation reaction in the assays.

Table 2 IC₅₀ values of dual-target compounds against *M. tuberculosis* LeuRS and MetRS

Compound number	R ¹	IC ₅₀ (μM)	
		<i>Mtb</i> LeuRS	<i>Mtb</i> MetRS
2	C ₆ H ₄ -4-NO ₂	5.8 ± 4.1 (3)	4.2 ± 1.3 (3)
3	C ₆ H ₄ -4-F	12.5 ± 4.7 (3)	10.7 ± 8.4 (4)
3a	CH ₃	95 ± 10 (2)	ND
4	C ₆ H ₃ -2,4-dCl	27.3 ± 1.3 (2)	22.7 ± 7.2 (3)
5	C ₆ H ₄ -3-NO ₂	8.9 ± 1.7 (2)	6.5 ± 0.4 (2)
5a	C ₆ H ₅	24.1 ± 5.5 (3)	37.5 ± 5.3 (3)
5b	CH ₃	38.4 ± 9.2 (3)	123 ± 15

The concentration of the compounds was varied in the range of 0.1 nM–500 μM. IC₅₀ values are reported as the mean ± standard deviation. The number of replicates is in parentheses. ND – not detectable.

bearing the methyl group instead of 2,4-dichlorophenyl, did not show any inhibition of either *Mtb*LeuRS or *Mtb*MetRS in the primary screen (Table 1). Compounds 5a and 5b with an R¹ phenyl and methyl group, respectively, demonstrated markedly increased IC₅₀ values when compared to compound 5, especially against *Mtb*MetRS. Both derivatives, though exhibit robust inhibitory activity, suggesting that the 3-nitrophenyl moiety does not play a crucial role as an R¹ substituent. This notion is supported by the marginal to absent activity of compounds 6 and 7 in the primary screen (Table 1). Combined with IC₅₀ data for previously reported derivatives,²⁰ our findings suggest that the phenyl group with a halogen atom or NO₂ group in the *para*-position as an R¹ substituent provides a substantial improvement in the ability of *N*-benzylidene-*N'*-thiazol-2-yl-hydrazine derivatives to inhibit both *Mtb*LeuRS and *Mtb*MetRS.

The potency of compounds 2–5 was tested against *Mtb* cultures with the H37Rv laboratory strain to determine the minimum inhibitory concentration (MIC). Cell cultures were incubated for a total of 14 days in parallel under four

different growth conditions consisting of Middlebrook 7H9-based media supplemented with either glucose or cholesterol/dipalmitoyl phosphatidylcholine (DPPC) as a carbon source in the presence or absence of 5% bovine serum albumin fraction V (BSA). All growth media contained 0.05% Tyloxapol as a surfactant with BSA-free media containing 0.3% Bacto casitone. MIC1 and MIC2 values were generated after incubation for 7 and 14 days, respectively (Table 3). Compounds 2, 4 and 5 exhibited no significant inhibitory activity against *Mtb* at concentrations below 50 μM. The level of inhibition needed for both *Mtb*LeuRS and *Mtb*MetRS that results in growth cessation is not known. This lack of whole cell activity is perhaps not surprising given that the IC₅₀ values for enzymatic inhibition are in the range of 4–22 μM. The cytosolic concentrations of these compounds would depend on the balance of uptake and efflux as well as compound metabolism by the pathogen. In contrast, compound 3 was found to exert potent inhibition of cells, exhibiting whole cell growth inhibition as observed from its MIC values which were noticeably lower than the IC₅₀ values for on-target inhibition, suggesting that compound 3 could inhibit additional targets. This suggestion is supported by the carbon source selectivity of compound 3 as demonstrated by the more than 10-fold increased potency against the pathogen growing in media containing glucose as opposed to cholesterol/DPPC as the major carbon source. Thus, careful validation of intracellular targets of compound 3 is required.

We subsequently examined compound 3 for toxicity against human cells. The *in vitro* cytotoxic activity of the compound was evaluated by the MTT assay against the human embryonic kidney 293 cell line (HEK293) and the human hepatocellular carcinoma cell line (HepG2) following procedures described previously.³⁰ Compound 3, tested in the concentration range of 6.25–100 μM, demonstrated CC₅₀ (concentration to cause 50% cytotoxicity) values greater than 100 μM, exhibiting low toxicities to human cell lines (ESI† Table S2). This indicates the mycobacteria-selective inhibitory potency of the compound.

Experimental

The general procedure of *N*-benzylidene-*N'*-thiazol-2-yl-hydrazine derivative synthesis and ¹H NMR, ¹³C NMR and HPLC-MS data for compounds 3–37, 3a, 5a, and 5b are provided in the ESI.†

Molecular docking

The receptor–ligand flexible docking was performed using the DOCK program.^{31–34} As a receptor, we used the homology model of *M. tuberculosis* LeuRS, which was obtained by us earlier,²⁰ and crystal structure of *M. tuberculosis* MetRS (PDB ID: 6AX8). Ligand geometry was calculated using the YFF force field.³⁵ Partial atomic charges of the ligands were added with the Kirchhoff method.³⁶

Docking parameters have been set as described previously,³⁷ except for several parameters. In our

Table 3 Inhibitory activity of the compounds against *M. tuberculosis* H37Rv cell growth

Compound number	MIC (μM)							
	Medium A		Medium B		Medium C		Medium D	
	MIC1	MIC2	MIC1	MIC2	MIC1	MIC2	MIC1	MIC2
2	50	≥ 50	50	> 50	> 50	> 50	≥ 50	> 50
3	1.56	2.3	19	37	0.78	2.3	9.4	25
4	> 50	> 50	> 50	> 50	> 50	> 50	> 50	> 50
5	> 50	> 50	≥ 50	> 50	37	> 50	37	50
Isoniazid	0.1	0.3	0.6	0.6	0.07	0.1	0.39	0.39

MIC1 and MIC2 were generated after incubation for 7 and 14 days, respectively. Medium A: 7H9/glucose/BSA/Tyloxapol. Medium B: 7H9/DPPC/cholesterol/BSA/Tyloxapol. Medium C: 7H9/glucose/casitone/Tyloxapol. Medium D: 7H9/DPPC/casitone/Tyloxapol.

experiments, the active site atoms included the atoms of amino acid residues selected within 8 Å from the reference ligand. The active site spheres for the ligand docking were calculated with the DOCK sphgen software. The spheres which were outside of the active site were deleted manually. Grid maps were calculated using the program Grid, with a grid spacing of 0.3 Å. Proteins were represented by an all atom model. In our virtual screening experiments, the 'multiple anchors' parameter was chosen, the minimum of heavy atoms in the anchor was set to 6, and the maximum number of orientations was 1000.

The superposition of the active sites of *M. tuberculosis* LeuRS and MetRS was analyzed using Discovery Studio Visualizer.³⁸ The amino acids of the MetRS active site were used as a template during molecular overlay. The parameters for superposition were set as the following: align by field: 50% steric, 50% electrostatic. The RMSD of superposition was 0.73.

Docking data for compounds 1–37 could be found in the ESI.†

Cloning of *M. tuberculosis* MetRS

The gene encoding MetRS was isolated from the genomic DNA of *M. tuberculosis* H37Rv (National Institute of Phthisiology and Pulmonology named after F.G. Yanovsky of the NAMS of Ukraine, Kyiv). For the His₆-MetRS construct, primers MetRSMt-N (5'-CCA TGG AGC CCT ATT ACG TCA CCA CCG CG) and MetRSMt-C (5'-AAG CTT GCC TTC GGG TGG TTG CGG CGG CTG G) were designed according to the NCBI reference sequence NC_000962.3. Appropriate sites for NcoI and HindIII restriction enzymes were included into MetRSMt-N and MetRSMt-C, respectively. Cloning into a final expression vector was done by isolating the NcoI-HindIII fragment and ligating it into NcoI-HindIII digested *E. coli* expression plasmid pET28b. Resulting plasmid pET28b/MetRS was transformed into *E. coli* BL21 (DE3) Star cells (Invitrogen).

Purification of *M. tuberculosis* MetRS and LeuRS

For the production of C-terminally tagged His₆ derivative of *M. tuberculosis* MetRS (*Mtb*MetRS), the cells were grown in LB medium supplemented with 3% v/v ethanol, and the expression was induced with 0.1 mM isopropyl- β -D-

thiogalactopyranoside for 5 hours at 16 °C. The cells from 1 L culture were harvested and sonicated in 8–10 mL of a lysis buffer (50 mM Tris-HCl, pH 8.0 at 25 °C, 300 mM NaCl, 10% v/v glycerol, 0.5 mM phenylmethylsulfonyl fluoride, 0.5% v/v Triton X-100) containing protease inhibitors (cOmplete, EDTA-free protease inhibitor cocktail tablet; Roche Applied Science). The cell debris was removed by centrifugation at 10 000g for 25 min. His₆-MetRS was purified by a standard procedure employing affinity chromatography on Ni²⁺-nitroacetic acid (Ni-NTA) Sepharose Fast Flow resin (GE Healthcare). Briefly, the cell-free extract was supplemented with imidazole to a final concentration of 15 mM and combined with 2 ml Ni-NTA Sepharose Fast Flow resin equilibrated in the lysis buffer supplemented with 15 mM imidazole. After extensive washing with the same buffer, His₆-MetRS was eluted with a lysis buffer containing 250 mM imidazole. The fractions containing His₆-MetRS (judged by Coomassie Brilliant Blue staining after SDS-PAGE) were pooled and further purified by size-exclusion chromatography on a Hi-Load 16/60 Superdex 200 (150 mL, Pharmacia Biotech) column, equilibrated with 50 mM HEPES-NaOH at pH 7.0, 10 mM β -mercaptoethanol, 100 mM NaCl, 10% v/v glycerol, and 0.003% w/v NaN₃, with a flow rate of 1 mL min⁻¹. The purified protein was concentrated to 3.75 mg mL⁻¹ and stored at -80 °C.

Mycobacterium tuberculosis LeuRS cloned into the pET28a vector was a generous gift from Stephen Cusack and Andres Palencia. The enzyme was expressed in *E. coli* and purified as described previously.²⁰

The final purity of proteins was monitored by SDS-PAGE and UV spectroscopy. Protein concentrations were determined by the Bradford assay³⁹ using Roti® Quant (Roth).

*Mtb*LeuRS and *Mtb*MetRS inhibition studies

All the tested compounds but one were dissolved in 100% DMSO (Merck) to a concentration of 10 mM. The stock solution of compound 25 was at a concentration of 5 mM.

Assays were conducted at 25 °C in clear, flat bottom, polystyrene, 96-well plates.

Each assay was performed in a 50 μL reaction volume consisting of 100 mM HEPES-NaOH, pH 7.5, 10 mM MgCl₂,

15 mM KCl, 1 mM DTT, 50 $\mu\text{g mL}^{-1}$ BSA (for *MtbLeuRS*) or 50 mM HEPES–NaOH, pH 7.5, 15 mM MgCl_2 , 10 mM KCl, 0.5 mM DTT, 10 $\mu\text{g mL}^{-1}$ BSA (*MtbMetRS* standard reaction buffer) supplemented with 200 μM ATP (Sigma), 1 mg mL^{-1} total *E. coli* MRE 600 tRNA (Boehringer Mannheim), 50 nM *MtbLeuRS* or *MtbMetRS*, cognate amino acid (1 mM leucine (Sigma) or 0.5 mM methionine (Pierce), respectively) and 0.25 U mL^{-1} yeast inorganic pyrophosphatase (iPPase; Sigma). Each compound at the desired concentrations (2.5 μL in 100% DMSO) was incubated with one of the enzymes in 25 μL of appropriate reaction buffer for 30 min before the aminoacylation reaction was initiated by the addition of a 25 μL mix of ATP, cognate amino acid, tRNA and iPPase in the same reaction buffer. After a 10 min incubation, the reaction was stopped by the addition of 100 μL BIOMOL® GREEN reagent (Enzo Life Science). The signal of BIOMOL® GREEN reagent was developed for 30 min at 25 °C and the absorbance was read at 630 nm using a Biotek ELx800™ (Biotek) plate reader.

Data points were normalized to a percentage:

Inhibition (%)

$$= \left[1 - \frac{(\text{OD}_{630}(\text{Sample}) - \text{OD}_{630}(\text{Blank}))}{\text{Avg}\{\text{OD}_{630}(\text{Control}) - \text{OD}_{630}(\text{Blank})\}} \right] \times 100$$

The blank and control wells contained 2.5 μL 100% DMSO instead of a compound. The blank wells also lacked an aminoacyl-tRNA synthetase. The IC_{50} values were calculated using nonlinear regression (sigmoidal logistic curve) from Origin 6.0. The processed data may be found in the ESI.†

The impact of compounds on reactions downstream of the aminoacylation reaction was monitored in two sets of control assays.

Set 1. Assays of iPPase activity were performed in 50 μL *MtbMetRS* standard reaction buffer supplemented with 5 μM inorganic pyrophosphate and 50 μM inhibitor. Inorganic PPase was present at a concentration of 0.25 U mL^{-1} . The reaction was initiated by the addition of enzyme, allowed to proceed for 10 min and stopped by the addition of 100 μL BIOMOL® GREEN reagent, followed by processing and analysis as described above. Control and blank incubations were conducted with DMSO only. The blank wells lacked enzymes.

Set 2. To measure the compounds' impact on the development of BIOMOL® GREEN signal, 100 μL reagent was added to 50 μL *MtbMetRS* standard reaction buffer supplemented with 10 μM phosphate standard (Enzo Life Sciences) and 50 μM inhibitor. After 30 min, the incubation absorbance was read at 630 nm and analysed. The blank and control wells contained DMSO only. In the blank wells, the phosphate standard was absent.

Determination of minimum inhibitory concentrations (MICs)

Minimum inhibitor concentrations (MICs) were determined in four Middlebrook 7H9-based media: 7H9/glucose/BSA/

Tyloxapol (4.7 g L^{-1} 7H9 broth base, 5 g L^{-1} BSA, 4 g L^{-1} glucose, 0.81 g L^{-1} NaCl, 0.5 ml L^{-1} Tyloxapol); 7H9/DPPC/cholesterol/BSA/Tyloxapol (4.7 g L^{-1} 7H9 broth base, 5 g L^{-1} BSA, 5 mg L^{-1} DPPC, 0.062 mM cholesterol, 0.81 g L^{-1} NaCl, 0.5 ml L^{-1} Tyloxapol); 7H9/glucose/casitone/Tyloxapol (4.7 g L^{-1} 7H9 broth base, 0.3 g L^{-1} Bacto casitone, 4 g L^{-1} glucose, 0.81 g L^{-1} NaCl, 0.5 ml L^{-1} Tyloxapol); 7H9/DPPC/casitone/Tyloxapol (4.7 g L^{-1} 7H9 broth base, 0.3 g L^{-1} Bacto casitone, 14 mg L^{-1} DPPC, 0.81 g L^{-1} NaCl, 0.5 ml L^{-1} Tyloxapol). The compounds were serially diluted in required medium two-fold across wells in 96-well clear round-bottom plates, plated in duplicates. Isolated *Mtb* cells (ATCC 27294) were grown to an OD_{600} of 0.2–0.3 in the required medium and diluted 10^3 -fold in the same medium. Then, 50 μL was added to each well of the compound-containing plates, approximating 10^4 cells per well in a total volume of 100 μL per well giving a final compound concentration range of 0.049–50 μM . Isoniazid and DMSO (drug-free) were used as positive and negative controls, respectively. All plates were incubated for a total of 14 days at 37 °C in zip-lock bags. At 7 and 14 days, cell growth was estimated using an inverted enlarging mirror plate reader with the MIC taken as the lowest compound concentration that inhibited all visible growth. At 14 days, 10 μL Alamar Blue was added to each well in plates with the Middlebrook 7H9 regular medium and those with the cholesterol medium. The plates were incubated at 37 °C for 24 hours and read using visual scoring to distinguish cholesterol precipitation from growths which occur if the media cooled down during the MIC set-up.

In vitro cytotoxicity assay

The human embryonic kidney 293 cell line (HEK293) was obtained from the Russian Cell Culture Collection (Institute of Cytology of the Russian Academy of Science, St. Petersburg, Russia). The human hepatocellular carcinoma cell line (HepG2) was obtained from the Bank of Cell Lines from human and animal tissue (R. E. Kavetsky Institute of Experimental Pathology, Oncology and Radiobiology, NAS of Ukraine, Kyiv, Ukraine). HEK293 and HepG2 cell viability was examined by MTT assay as described previously.³⁰ Viable cells were dispensed into a 96-well tissue plate at ~5000 cells per well (HEK293) or ~ 10^4 cells per well (HepG2), incubated for 24 hours, and then treated with a compound at a final concentration range of 6.25–100 μM . After a 72 hour treatment, the cells were processed with MTT (3-(4,5-dimethyl-thiazol-2-yl)-2,5-diphenyl-tetrazolium bromide; Sigma). The cell viability was expressed as a percentage relative to the untreated control cells.

Conclusions

In this work, we provide the first attempt to achieve simultaneous targeting of two AARSs by a single small molecular inhibitor. Considering the structural resemblance in aminoacyl-adenylate binding sites of the two enzymes, *M. tuberculosis* LeuRS and MetRS, and using the chemical

scaffold of known *Mtb*LeuRS inhibitors, *N*-benzylidene-*N*-thiazol-2-yl-hydrazines, we identified four compounds that exhibited dual on-target activity as demonstrated by their IC₅₀ values in enzymatic activity assays. The hit compound 3 showed anti-tubercular whole cell activity against *Mtb* H37Rv in *in vitro* bioassays as well as low cytotoxicity to HEK293 and HepG2 human cell lines. Our findings suggest that the compound is valuable for further biological evaluation, including the determination of its on- and potentially off-target effects in *Mtb*, and the frequency of resistance of *Mtb* H37Rv against the compound as well as the activity of the compound against drug-resistant clinical isolates of *Mtb*.

Conflicts of interest

The authors declare no conflicts of interest from a financial or commercial standpoint.

Acknowledgements

This work was supported by the Science and Technology Center in Ukraine (contract No. 6258) and by the Intramural Research Program of NIH, NIAID (AI000693-25). The authors are grateful to Dr. Stephen Cusack and Dr. Andres Palencia (EMBL Grenoble Outstation, France) for the gift of plasmid encoding *M. tuberculosis* LeuRS. We also thank Prof. Vasyly Mel'nyk (National Institute of Phthisiology and Pulmonology named after F.G. Yanovsky of the NAMS of Ukraine, Kyiv, Ukraine) for providing the genomic DNA of *M. tuberculosis* H37Rv. We are indebted to Anna Iatsyshyna, Institute of Molecular Biology and Genetics NAS Ukraine, for helping with cytotoxicity tests. We are grateful to Dr. Clifton Barry III (National Institute of Allergy and Infectious Disease, National Institute of Health, Maryland, USA) for his continued interest and support.

Notes and references

- M. D. J. Libardo, H. I. Boshoff and C. E. Barry 3rd, *Curr. Opin. Pharmacol.*, 2018, **42**, 81.
- S. F. K. Lee, B. E. Laughon, T. D. McHugh and M. Lipman, *Curr. Opin. Pulm. Med.*, 2019, **25**, 271.
- E. Torfs, T. Piller, P. Cos and D. Cappoen, *Int. J. Mol. Sci.*, 2019, **20**, 2868.
- K. Li, L. A. Shurig-Briccio, X. Feng, A. Upadhyay, V. Pujari, B. Lechartier, F. L. Fontes, H. Yang, G. Rao, W. Zhu, A. Gulati, J. H. No, G. Cintra, S. Bogue, Y. L. Liu, K. Molohon, P. Orlean, D. A. Mitchell, L. Freitas-Junior, F. Ren, H. Sun, T. Jiang, Y. Li, R. T. Guo, S. T. Cole, R. B. Gennis, D. C. Crick and E. Oldfield, *J. Med. Chem.*, 2014, **57**, 3126.
- A. L. Hopkins, *Nat. Chem. Biol.*, 2008, **4**, 682.
- G. H. M. Vondenhoff and A. Van Aerschot, *Eur. J. Med. Chem.*, 2011, **46**, 5227.
- Y. L. Pang, K. Poruri and S. A. Martinis, *Wiley Interdiscip. Rev.: RNA*, 2014, **5**, 461.
- V. Dewan, J. Reader and K. M. Forsyth, *Top. Curr. Chem.*, 2014, **344**, 293.
- J. M. Ho, E. Bakkalbasi, D. Söll and C. A. Miller, *RNA Biol.*, 2018, **15**, 667.
- C. S. Francklyn and P. Mullen, *J. Biol. Chem.*, 2019, **294**, 5365.
- G. Eriani, M. Delarue, O. Poch, J. Gangloff and D. Moras, *Nature*, 1990, **347**, 203.
- C. P. Randall, D. Rasina, A. Jirgensons and A. J. O'Neill, *Antimicrob. Agents Chemother.*, 2016, **60**, 6359.
- P. O'Donoghue and Z. Luthey-Schulten, *Microbiol. Mol. Biol. Rev.*, 2003, **67**, 550.
- S. English, U. English, F. von der Haar and F. Cramer, *Nucleic Acids Res.*, 1986, **14**, 7529.
- T. L. Lincecum and S. A. Martinis, *SAAS Bull. Biochem. Biotechnol.*, 2000, **13**, 25.
- H. Jakubowski, *Acta Biochim. Pol.*, 2011, **58**, 149.
- N. Cveticic, A. Palencia, I. Halasz, S. Cusack and I. Gruic-Sovulj, *EMBO J.*, 2014, **33**, 1639.
- M. Bilus, M. Semanjski, M. Mocibob, I. Zivkovic, N. Cveticic, D. S. Tawfik, A. Toth-Petroczy, B. Macek and I. Gruic-Sovulj, *J. Mol. Biol.*, 2019, **431**, 1284.
- G. B. Fortowsky, D. J. Simard, M. M. Aboelnga and J. W. Gauld, *Biochemistry*, 2015, **54**, 5757.
- O. I. Gudzera, *et al.*, *Bioorg. Med. Chem. Lett.*, 2016, **24**, 1023.
- W. Huang, *et al.*, *Bioorg. Med. Chem. Lett.*, 2017, **27**, 2702.
- T. Hussain, M. Yogavel and A. Sharma, *Antimicrob. Agents Chemother.*, 2015, **59**, 1856.
- R. M. Ranade, Z. Zhang, J. R. Gillespie, S. Shibata, C. L. Verlinde, W. G. Hol, E. Fan and F. S. Buckner, *Antimicrob. Agents Chemother.*, 2015, **59**, 7128.
- L. S. Torrie, S. Brand, D. A. Robinson, E. J. Ko, L. Stojanovski, F. R. C. Simeons, S. Wyllie, J. Thomas, L. Ellis, M. Osuna-Cabello, O. Epemolu, A. Nühs, J. Riley, L. MacLean, S. Manthri, K. D. Read, I. H. Gilbert, A. H. Fairlamb and M. De Rycker, *ACS Infect. Dis.*, 2017, **3**, 718.
- R. L. Jarvest, J. M. Berge, V. Berry, H. F. Boyd, M. J. Brown, J. S. Elder, A. K. Forrest, A. P. Fosberry, D. R. Gentry, M. J. Hibbs, D. D. Jaworski, P. J. O'Hanlon, A. J. Pope, S. Rittenhouse, R. J. Sheppard, C. Slater-Radosti and A. Worby, *J. Med. Chem.*, 2002, **45**, 1959.
- A. G. Eissa, J. A. Blaxland, R. O. Williams, K. A. Metwally, S. M. El-Adl, El-S. M. Lashine, L. W. Baillie and C. Simons, *J. Enzyme Inhib. Med. Chem.*, 2016, **31**, 1694.
- S. Robles, Y. Hu, T. Resto, F. Dean and J. M. Bullard, *Curr. Drug Discovery Technol.*, 2017, **14**, 156.
- X. Barros-Álvarez, S. Turley, R. M. Ranade, J. R. Gillespie, N. A. Duster, C. L. M. J. Verlinde, E. Fan, F. S. Buckner and W. G. J. Hol, *Acta Crystallogr., Sect. F: Struct. Biol. Commun.*, 2018, **74**, 245.
- W. Wang, B. Qin, J. A. Wojdyla, M. Wang, X. Gao and S. Cui, *IUCrJ*, 2018, **5**, 478.
- G. Volynets, S. Lukashov, I. Borysenko, A. Gryshchenko, S. Starosyla, V. Bdzholia, T. Ruban, A. Iatsyshyna, L. Lukash, Ya. Bilokin and S. Yarmoluk, *Monatsh. Chem.*, 2019, DOI: 10.1007/s00706-019-02493-5.
- B. K. Stoichet, R. M. Stroud, D. V. Santi, I. D. Kuntz and K. M. Perry, *Science*, 1993, **259**, 1445.

- 32 D. L. Bodian, R. B. Yamasaki, R. L. Buswell, J. F. Stearns, J. M. White and I. D. Kuntz, *Biochemistry*, 1993, **32**, 2967.
- 33 C. S. Ring, E. Sun, J. H. McKerrow, G. K. Lee, P. J. Rosenthal, I. D. Kuntz and F. E. Cohen, *Proc. Natl. Acad. Sci. U. S. A.*, 1993, **90**, 3583.
- 34 T. J. Ewing, S. Makino, A. G. Skillman and I. D. Kuntz, *J. Comput.-Aided Mol. Des.*, 2001, **15**, 411.
- 35 O. Ya. Yakovenko, A. A. Oliferenko, A. G. Golub, V. G. Bdzhola and S. M. Yarmoluk, *Ukr. Bioorg. Acta*, 2007, **1**, 52.
- 36 O. Ya. Yakovenko, A. A. Oliferenko, V. G. Bdzhola, V. A. Palyulin and N. S. Zefirov, *J. Comput. Chem.*, 2008, **29**, 1332.
- 37 B. D. Bursulaya, M. Totrov, R. Abagyan and C. L. Brooks III, *J. Comput.-Aided Mol. Des.*, 2003, **17**, 755.
- 38 Discovery Studio Visualizer 4.0. <https://www.3dsbiovia.com/products/collaborative-science/biovia-discovery-studio/visualization-download.php>, (accessed May 2019).
- 39 M. M. Bradford, *Anal. Biochem.*, 1976, **72**, 248.